

# Synthesis of Chiral Bifunctional NHC Ligands and Survey of Their Utilities in Asymmetric Gold Catalysis

Jun-Qi Zhang,<sup>†,‡</sup> Yunkui Liu,<sup>†,§</sup> Xing-Wang Wang,<sup>‡,§</sup> and Liming Zhang<sup>\*,†,§</sup>

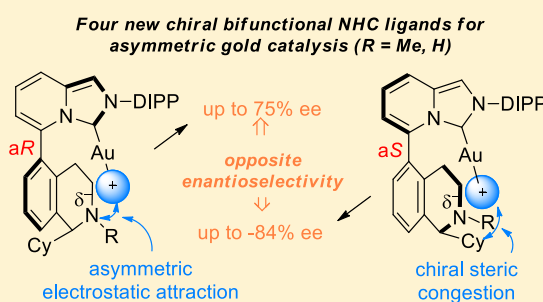
<sup>†</sup>Department of Chemistry and Biochemistry, University of California, Santa Barbara, California 93106, United States

<sup>‡</sup>Key Laboratory of Organic Synthesis of Jiangsu Province, College of Chemistry, Chemical Engineering and Materials Science, Soochow University, Suzhou 215123, P. R. China

<sup>§</sup>State Key Laboratory Breeding Base of Green Chemistry-Synthesis Technology, Zhejiang University of Technology, Hangzhou 310014, P. R. China

## S Supporting Information

**ABSTRACT:** The synthesis and characterization of the chiral bifunctional NHC ligands based on the imidazo[1,5-*a*]pyridine (ImPy) scaffold are described. These ligands possess a fluxional biaryl axis and a chiral center. The configurational stability of the biaryl axis in their gold(I) complexes is investigated. The application of these axially chiral ImPy-based AuCl complexes in a series of gold catalysis is explored, and varying degrees of asymmetric induction are observed. In most cases, the ligand (a*S,R*)-L8-H with its cyclohexyl group pointing to the reaction site and hence exerting asymmetric steric influence is more effective in asymmetric induction.



## INTRODUCTION

For the past several years, our lab has developed several remotely functionalized biaryl-2-ylphosphines [i.e., WangPhos and L1–L7 (Figure 1)] for gold catalysis.<sup>1</sup> These novel ligands feature a basic substituent at the bottom half of the pendant aryl ring. Because of the approximately linear arrangement of the P–Au–substrate coordination and the restricted rotation of the P–C2 bond imposed by the bulky adamantyl groups, they enable beneficiary second-coordination sphere interac-

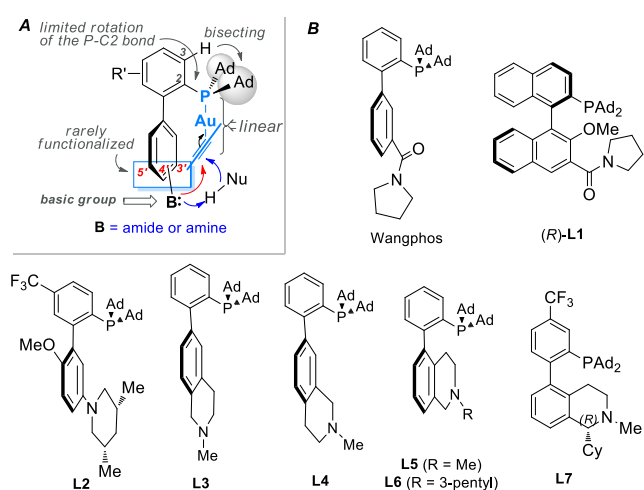
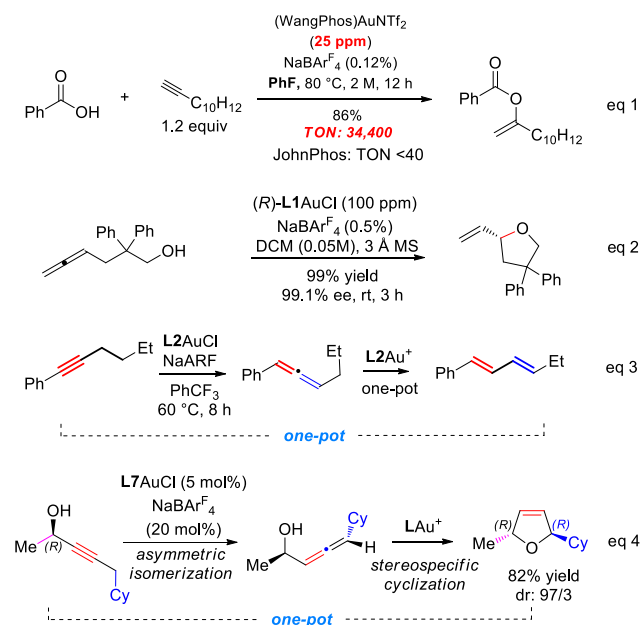


**Figure 1.** Novel biaryl-2-ylphosphines featuring a remote basic functional group specifically designed for homogeneous gold catalysis: (A) design and (B) a selected list of our reported ligands.

tions between the basic group and substrates and/or nucleophiles in homogeneous gold catalysis (Figure 1A). As such, a range of versatile and/or new gold catalyses have been developed.<sup>1</sup> For example, WangPhos, the first ligand of this type and one that features a 3'-carboxamide, can accelerate the gold-catalyzed addition of carboxylic acid to alkyne >800-fold by comparison to JohnPhos, a ligand of similar steric and electronic characteristics but without the remote basic group (eq 1).<sup>1i</sup> As a result, the loading of the gold catalyst in this reaction mixture can be decreased to a level of tens of parts per million. This accelerative gold catalysis is also applied to achieve for the first time accelerative asymmetric gold catalysis, in which hexa-4,5-dien-1-ols are cyclized with an excellent enantiomeric excess in the presence of as little as 100 ppm of the chiral cationic gold(I) catalyst<sup>2</sup> prepared from the binaphthyl ligand (R)-L1 (eq 2).<sup>1e</sup> Replacing the amide group of WangPhos with a more basic aniline or tertiary amino group led to ligands L2–L7, among others, that are capable of engaging novel interactions with alkyne substrates via the basic groups and thereby enable gold catalysis<sup>1a–d,f,h</sup> that cannot be achieved by conventional ligands. The first study in this context is the isomerization of alkynes into 1,3-dienes (eq 3). In this case, the remote anilinic group ( $pK_a \sim 4$ ) of ligand L2 is capable of effectively deprotonating the propargylic C–H bond ( $pK_a > 30$ ) due to the synergistic Au(I) activation and the

**Special Issue:** Asymmetric Synthesis Enabled by Organometallic Complexes

**Received:** June 17, 2019

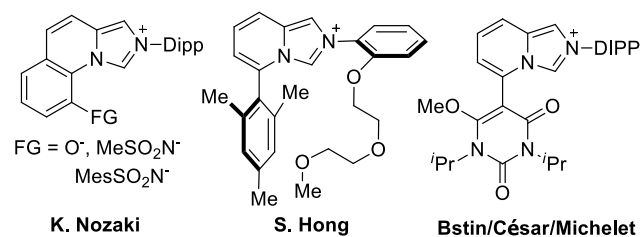


likely optimal ligand framework (eq 3). The extension of this synergistic soft propargylic deprotonation in the presence of the more basic tertiary amine-functionalized ligands led to, among other works,<sup>1b,d,f</sup> our recent report on asymmetric isomerization of propargylic alcohols into 2,5-dihydrofurans (eq 4).<sup>1a</sup> In this chemistry, chiral ligand L7 featuring a chiral tetrahydroisoquinoline and a fluxional axis can enable gold-catalyzed asymmetric isomerization of alkyne into chiral allene.

## RESULTS AND DISCUSSION

**Ligand Design.** Encouraged by these developments, we have recently extended the ligand design concept to the development of bifunctional NHC-type ligands and, in particular, their chiral versions based on the imidazo[1,5-*a*]pyridine framework (Figure 2). This class of NHC ligands (ImPy) was initially reported by Lassaletta<sup>3</sup> and Glorius<sup>4</sup>

### A. Some reported bifunctional ImPy ligands or ligand precursors



### B. New Chiral bifunctional ImPy ligands featuring a remote basic group vs. L7

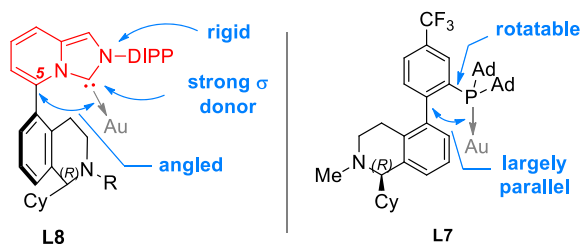
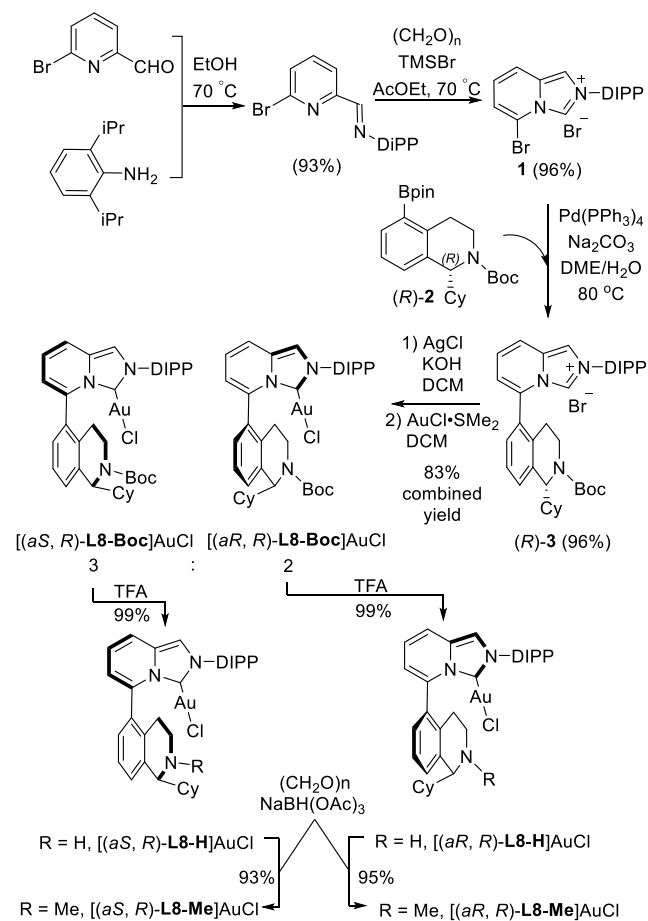


**Figure 2.** Bifunctional imidazo[1,5-*a*]pyridin-3-ylidene ligands or their precursors: (A) known examples and (B) our design and comparison to L7.

independently and has since been adopted for the preparation of Au(I)/Au(III) complexes with cytotoxicity<sup>5</sup> and photo-physical properties<sup>6</sup> and for structural considerations<sup>7</sup> and catalysis.<sup>7b,8</sup> Bifunctional ImPy ligands have also been developed for Au,<sup>8b</sup> Pd,<sup>9</sup> and Cu<sup>10</sup> chemistry (Figure 2A). Our design, as shown in Figure 2B, entails the installation of a chiral tetrahydroisoquinoline moiety at C-5 of the ligand imidazo[1,5-*a*]pyridine ring. The resulting ImPy ligand L8 should have a fluxional biaryl axis, where the two connecting aryl groups should be mostly oriented orthogonally. It is by design analogous to chiral phosphine ligand L7 but could offer three distinct differences (Scheme 1). (a) The NHC is more

### Scheme 1. Synthesis of [(*aS,R*)-L8-H]AuCl, [(*aS,R*)-L8-Me]AuCl, [(*aR,R*)-L8-H]AuCl, and [(*aR,R*)-L8-Me]AuCl



electron-donating and hence renders the cationic gold catalysts potentially more robust and offers a different catalytic activity profile. (b) The rigid imidazo[1,5-*a*]pyridine framework removes issues associated with C–P rotation in the phosphine case, including the necessity of installing bulky PAd<sub>2</sub> and the potential entropy penalty during reaction. (c) The carbene–Au–substrate line is tilted away from the pendant aryl ring due to the 5–6-fused nature of the top half of the ligand. We anticipate that the first two differences could offer discrete advantages to gold catalysis, but the third might diminish the second-coordination sphere interaction due to the increasing separation of the participating groups. Herein, we report the synthesis of several chiral ligands of this type, their characterizations, and a survey of their effectiveness in inducing asymmetric gold catalysis.

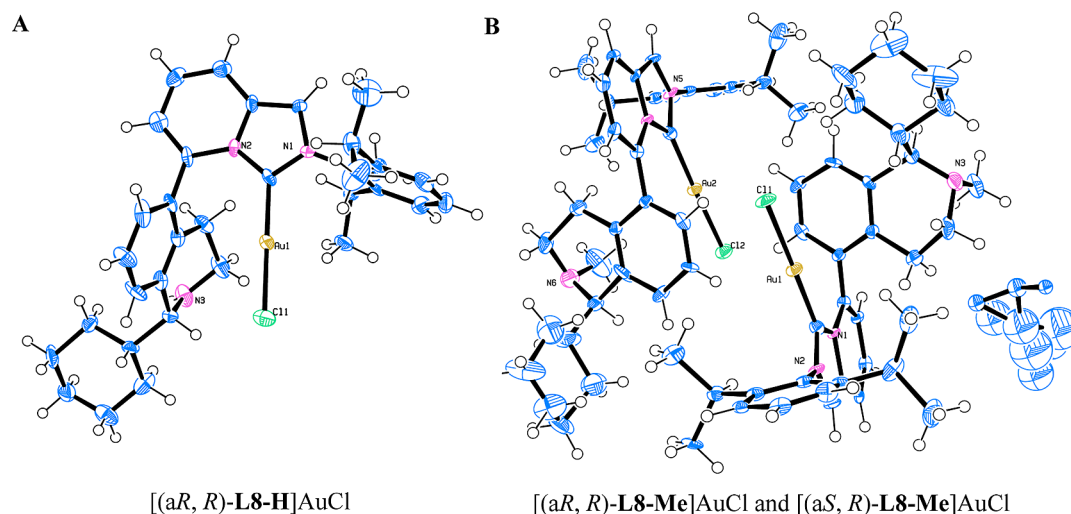


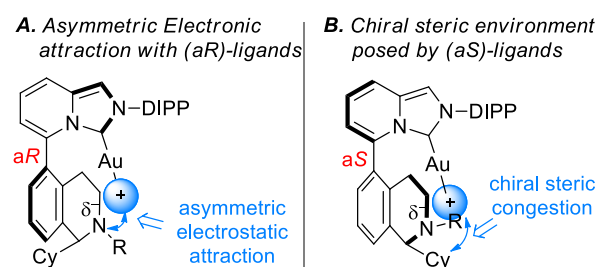
**Figure 3.** ORTEP drawings of [(aR,R)-L8-H]AuCl (A, solvent omitted) and [(aR,R)-L8-Me]AuCl and [(aS,R)-L8-Me]AuCl (B, solvent shown) showing 50% thermal ellipsoid probabilities. Selected bond distances (angstroms) and angles (degrees) for [(aR,R)-L8-H]AuCl: Au1–C1, 1.977(15); Au1–Cl1, 2.268(4); C1–N1, 1.352(19); C1–N2, 1.361(18); C7–C8, 1.45(2); C1–Au1–Cl1, 177.9(5); N1–C1–N2, 104.2(12). Selected bond distances (angstroms) and angles (degrees) for [(aR,R)-L8-Me]AuCl: Au2–C37, 2.00(3); Au2–Cl2, 2.294(8); C37–N4, 1.36(4); C37–N5, 1.37(3); C40–C44, 1.49(4); C37–Au2–Cl2, 178.3(9); N4–C37–N5, 99(2). Selected bond distances (angstroms) and angles (degrees) for [(aS,R)-L8-Me]AuCl: Au1–C1, 1.93(3); Au1–Cl1, 2.266(7); C1–N1, 1.39(4); C1–N2, 1.32(3); C4–C8, 1.47(4); C1–Au1–Cl1, 177.9(9); N1–C1–N2, 107(2).

### Synthesis of Chiral Bifunctional NHC Ligands and the Structural Data of Their Au(I) Complexes.

Our synthesis of the gold(I) complexes of (*R*)-L8 commenced with the condensation between 6-bromopicolinaldehyde and 2,6-diisopropylaniline, followed by the reaction with paraformaldehyde in the presence of TMSBr.<sup>11</sup> Upon workup, 5-bromo-2-(2,6-diisopropylphenyl)imidazo[1,5-*a*]pyridin-2-ium **1** was obtained as a white powder. Its Suzuki–Miyaura coupling with the boronate (*R*)-**2**, the synthesis of which we reported previously,<sup>1a</sup> yielded the biaryl NHC precursor salt (*R*)-**3** by employing a modified literature procedure.<sup>4</sup> The gold complex [(*R*)-L8-Boc]AuCl was prepared first by the synthesis of its silver complex as a crude product from (*R*)-**3** by using the combination of AgCl and KOH in dichloromethane in the dark and then by its transmetalation with AuCl·SMe<sub>2</sub>. As expected, [(*R*)-L8-Boc]AuCl exhibits a mixture of diastereomeric atropisomers (3:2 dr) due to the restricted rotation of the biaryl axis in the presence of AuCl. To our delight, they could be readily separated by regular silica gel flash column chromatography. Subsequently, the Boc groups of the separated NHC–Au(I) complexes [(aS,R)-L8-Boc]AuCl and [(aR,R)-L8-Boc]AuCl were quantitatively removed upon exposure to TFA at 0 °C, affording complexes [(aS,R)-L8-H]AuCl and [(aR,R)-L8-H]AuCl, respectively, as white solids upon subsequent aqueous NaHCO<sub>3</sub> washing. These solids are fully air and moisture stable. Furthermore, they underwent reductive amination in the presence of paraformaldehyde and NaBH(OAc)<sub>3</sub> without incident to smoothly deliver [(aS,R)-L8-Me]AuCl and [(aR,R)-L8-Me]AuCl, respectively, in excellent yields. Single crystals of [(aR,R)-L8-H]AuCl and of the 1:1 mixture of [(aR,R)-L8-Me]AuCl and [(aS,R)-L8-Me]AuCl were successfully cultivated and subsequently subjected to X-ray diffraction studies. Their molecular structures and selected structural data are shown in Figure 3. As expected, the C<sub>carbene</sub>–Au–Cl connection is nearly linear, with the angle ranging from 177.9° to 178.3°. The Au–Cl

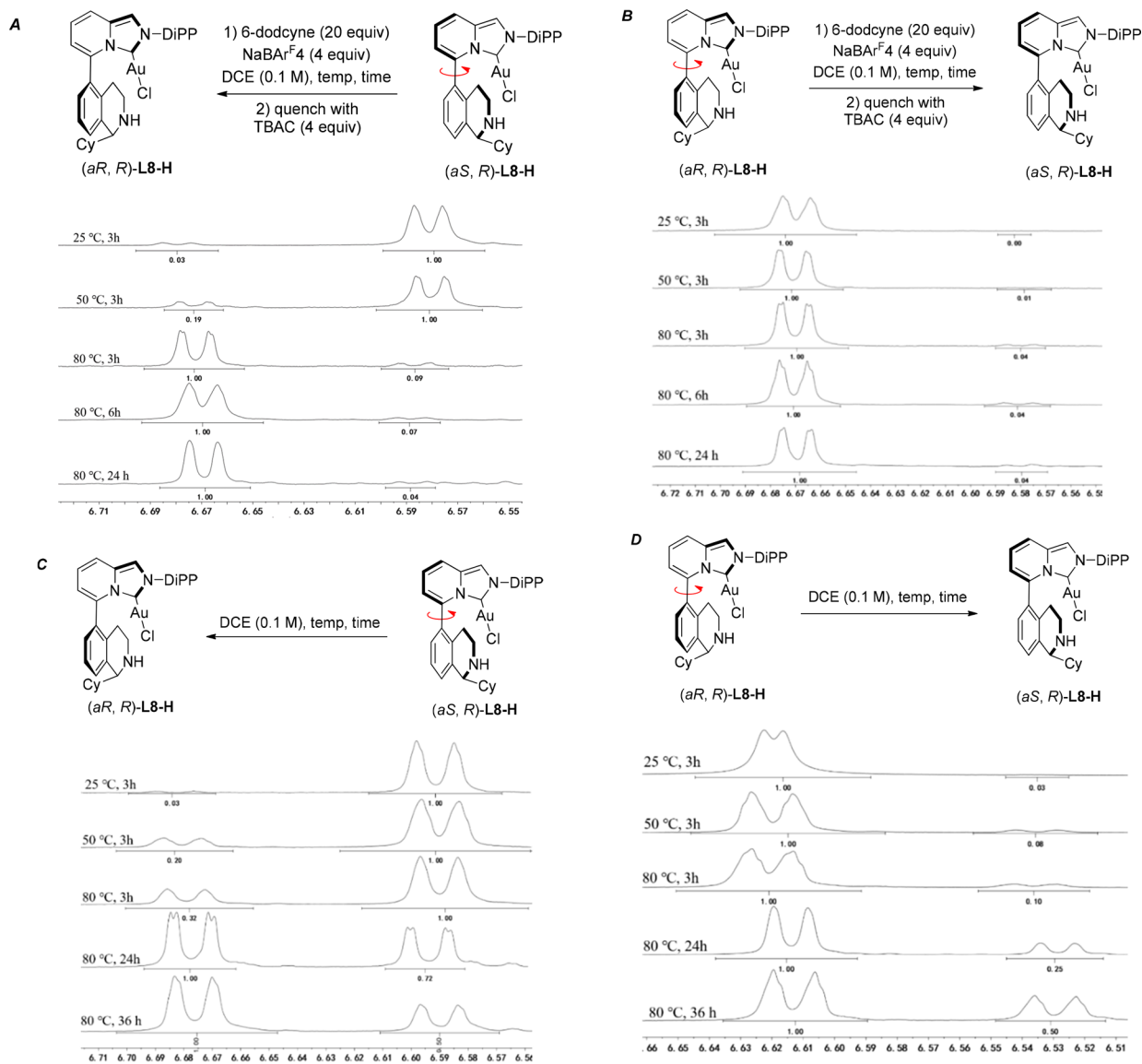
distances range from 2.266 to 2.294 Å, and their Au–carbene bond lengths range from 1.93 to 2.00 Å.

**Fluxional Nature of the Ligand Biaryl Axis.** Inspired by our previously reported work on the related phosphine ligands,<sup>1a</sup> we speculated that these chiral ImPy-based AuCl complexes, upon removal of the chloride, could rotate along its biaryl axis upon heating conditions. Thus, we first examined [(aS,R)-L8-H]AuCl using our previously employed protocol: heating a mixture of 1 equiv of the complex, 4 equiv of NaBARF<sub>4</sub>, and 20 equiv of 6-dodecyne in DCE at the specified temperature and then quenching the reaction with tetrabutylammonium chloride (4 equiv) after the specified time (Figure 4A). We note that this complex has the cyclohexyl group



**Figure 4.** Rationales for inducing chirality by the chiral bifunctional ImPy–Au complexes.

intrude into the space of AuCl. This protocol is intended to examine the biaryl axis fluxionality of the in situ-generated cationic [(aS,R)-L8-H]Au<sup>+</sup> complex. As shown in Figure 4A, a small amount of [(aR,R)-L8-H]AuCl was observed when the rotation was conducted at room temperature for 3 h. With a further increase in temperature to 50 °C, more [(aR,R)-L8-H]AuCl was detected with an (aR)/(aS) ratio of 0.19/1.00. The ratio increased to 1.00/0.09 when the conversion was performed at 80 °C for 3 h. Eventually, after 24 h, the (aR)/(aS) ratio was further increased to 1.00/0.04, which appears to be the equilibrium point. This conclusion was supported by

Scheme 2. Studying the Biaryl Axis Rotation of ImPy-Based Gold Complexes [(*R*)-L8-H]Au<sup>+</sup> and [(*R*)-L8-H]AuCl

reaching the same ratio when [(*aR*,*R*)-L8-H]AuCl was employed as the starting point (Figure 4B). This result confirms that the biaryl axis is indeed fluxional and is consistent with our previous observation, where the presumed cationic Au(I) intermediate with the cyclohexyl group pointing toward the gold center, i.e., with the (*aS*) configuration, is thermodynamically less stable than that with the (*aR*) configuration. We propose that the electrostatic attraction between cationic gold and the partially negatively charged and unhindered nitrogen in the case of the (*aR*) configuration is responsible for the difference in stability.

To our surprise, during the protracted cultivation of single crystals for X-ray studies, we detected epimerization of [(*R*)-L8-H]AuCl at its chiral axis in solution, which is in contrast to the configuration stability of L7AuCl.<sup>1a</sup> Subjecting either [(*R*)-L8-H]AuCl atropisomer in DCE to an elevated temperature confirmed it (Scheme 2C,D) and revealed (a) their rates of epimerization are similar to those of the cationic counterpart (i.e., Scheme 2A,B) and (b) the preference for the (*aR*) configuration over the (*aS*) configuration is only 2-fold, much lower than that of the cationic counterparts (~25-fold),

suggesting the predominating role of electronic attraction in favoring [(*aR*,*R*)-L8-H] in the cationic scenarios. We did not observe, however, that either atropisomer of [(*R*)-L8-H]AuCl in the solid state had undergone any epimerization while stored at 0 °C for 1 month.

**Applications in Asymmetric Gold Catalysis.** Having the four chiral ImPyAu(I) complexes in hand, we then survey their efficacy in enabling asymmetric gold catalysis,<sup>12</sup> albeit the semifluxional nature of their biaryl axes. It is surmised, as shown in Figure 4A, that with (*aR*,*R*)-L8-H as the ligand, the electrostatic attraction between the partially negatively charged ligand nitrogen and the cationic intermediates ubiquitous in gold catalysis might introduce the necessary asymmetric interaction to effectively induce product chirality. Alternatively, as shown in Figure 4B, the chiral steric environment posed by the protruding cyclohexyl group in the case of (*aS*,*R*)-L8-H could likewise be conducive to asymmetric catalysis.

We first investigated the gold-catalyzed alkoxylation of 1,6-enyne **4a** [X = C(CO<sub>2</sub>Me)<sub>2</sub>],<sup>13</sup> and the results are summarized in Table 1 (entries 1–6). With [(*aR*,*R*)-L8-H]AuCl as the catalyst precursor and AgSbF<sub>6</sub> as the chloride

Table 1. Au-Catalyzed Alkoxy cyclization of 1,6-Enynes<sup>a</sup>

4a: X = C(CO<sub>2</sub>Me)<sub>2</sub>  
4b: X = NTs

5a: X = C(CO<sub>2</sub>Me)<sub>2</sub>  
5b: X = NTs

entry	enyne	catalyst	chloride scavenger	yield <sup>b</sup> (%)	ee <sup>c</sup> (%)
1	4a	[(aR,R)-L8-H] AuCl	AgSbF <sub>6</sub>	52	33
2	4a	[(aR,R)-L8-Me] AuCl	AgSbF <sub>6</sub>	trace	–
3	4a	[(aS,R)-L8-H] AuCl	AgSbF <sub>6</sub>	99	–73
4	4a	[(aS,R)-L8-Me] AuCl	AgSbF <sub>6</sub>	99	–66
5	4a	[(aS,R)-L8-H] AuCl	NaBAR <sup>F</sup> <sub>4</sub>	82	–18
6	4a	[(aS,R)-L8-H] AuCl	[Ag(CH <sub>3</sub> CN) <sub>2</sub> ] <sup>+</sup> BARF <sup>–</sup>	97	–77
7	4b	[(aS,R)-L8-H] AuCl	AgSbF <sub>6</sub>	trace	–
8	4b	[(aR,R)-L8-H] AuCl	AgSbF <sub>6</sub>	71	21

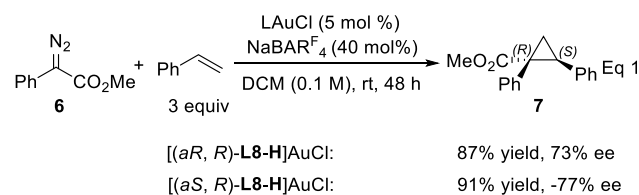
<sup>a</sup>Reaction conditions: 0.1 mmol scale, 5 mol % catalyst based on Au center, 5 mol % chloride scavenger, 1 mL of mixed solvent (1:1 DCM/MeOH). <sup>b</sup>Isolated yields. <sup>c</sup>Determined by chiral HPLC. The absolute stereochemistry is assigned upon the comparison of its specific rotation to the literature data, and the negative ee values indicate the opposite configuration of the product.

scavenger, desired product **5a** was formed in 52% yield and with 33% ee (entry 1). On the other hand, the *N*-methyl counterpart of [(aR,R)-L8-H]AuCl, i.e., [(aR,R)-L8-Me]AuCl, led to only a trace amount of reaction (entry 2). Significant increases in enantioselectivity and yield in the presence of either of the (aS) ligands, i.e., [(aS,R)-L8-H] or [(aS,R)-L8-Me], were observed (entry 3 or 4, respectively). We note that the sense of chirality is opposite and the ee can reach a respectable value of –73%. The chloride scavenger appears to be important, as NaBAR<sup>F</sup><sub>4</sub> led to poor ee (entry 5) but [Ag(CH<sub>3</sub>CN)<sub>2</sub>]<sup>+</sup> BARF<sup>–</sup> improved it to –77% (entry 6). Because (R)-L8-H performed better than (R)-L8-Me, the former ligands were employed in the subsequent studies.

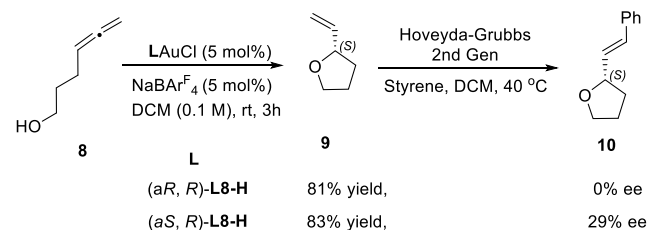
Sulfonamide substrate **4b**,<sup>11c,12</sup> however, reacted quite differently, with (aR,R)-L8-H performing instead much better than [(aS,R)-L8-H] in terms of reaction yield (entries 7 and 8), but the ee remained poor.

We then evaluated the asymmetric cyclopropanation of styrene by the gold carbene generated from methyl phenyldiazoacetate **6**. Despite this reaction has been widely reported by employing chiral Rh catalysts,<sup>14</sup> the gold counterpart<sup>15</sup> has not been achieved with good enantiomeric excess, despite success in related studies.<sup>16</sup> To our delight, both ligands (aS,R)-L8-H and (aR,R)-L8-H could promote the reaction with high efficiency and decent enantiomeric excess. The absolute stereochemistry of **7** is assigned upon the comparison of its specific rotation to the literature data.<sup>14</sup> Again, the ligand atropisomers led to the selective formation of the enantiomer of **7** and hence to the negative ee value (eq 5).

The asymmetric cyclizations of 4-allen-1-ol **8** was next examined. As shown in Scheme 3, [(aR,R)-L8-H]AuCl with its

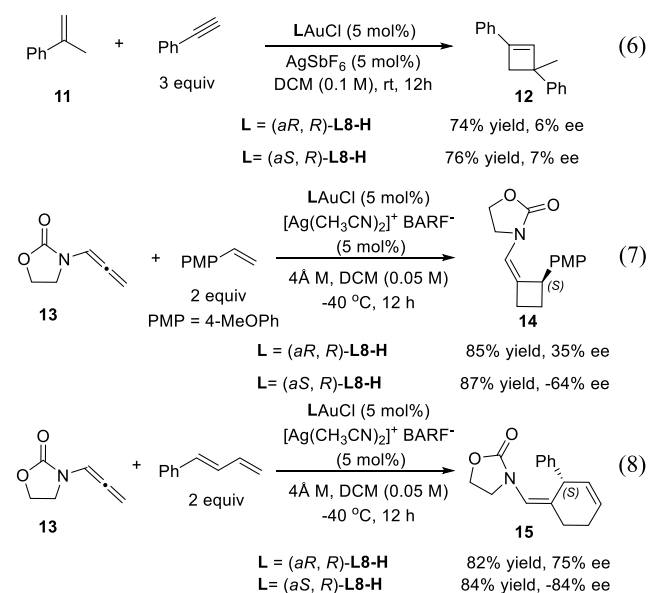


Scheme 3. Gold-Catalyzed Enantioselective Cyclization of 4-Allen-1-ol 7



cyclohexyl group pointing away from gold induced no chirality; on the other hand, its atropisomer [(aS,R)-L8-H]AuCl led to the formation of vinyltetrahydrofuran **9** with 29% ee, which was determined by chiral HPLC analysis of its cross-coupling product **10**. We previously reported that with a remotely amide-functionalized binaphthyl-2-ylphosphine as the ligand an accelerative asymmetric gold catalysis permits the cyclization of **8** with excellent ee.<sup>1c</sup> In that chemistry, the amide group, behaving as a general base, enables the drastic rate acceleration and thereby the asymmetric induction. The lack of such acceleration in the case of (aR,R)-L8-H is not entirely surprising as the basic nitrogen is most likely positioned too far from the HO group during cyclization.

The [2+2] cycloaddition between  $\alpha$ -methylstyrene and phenylacetylene has been realized asymmetrically by using non-C<sub>2</sub>-chiral Josiphos digold(I) complexes as the catalyst.<sup>17</sup> However, neither (aR,R)-L8-H nor (aS,R)-L8-H was able to induce much chirality in this reaction; however, the reaction was efficient (eq 6). Notably, in this case, the same enantiomer was preferred.

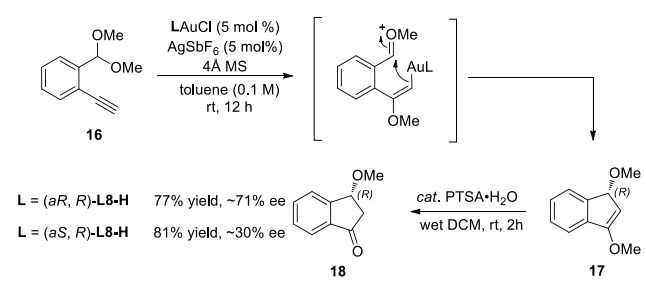


We next turned to the reactions of allenamides, which have been subjected to asymmetric gold catalysis in several

reports.<sup>18</sup> As shown in eq 7, both atropisomers of (*R*)-**L8-H** smoothly promoted the intermolecular [2+2] cycloaddition between allenamide **13** and *p*-methoxystyrene to afford the cyclobutane **14** in >80% yields. For the asymmetric induction, similar to the observations in Table 1, they led to opposite stereoselectivities and (*aS,R*)-**L8-H** was substantially better than its (*aR*) counterpart. The reaction of **13** with 1-phenyl-1,3-butadiene was the most enantioselective with either of the (*R*)-**L8-H** isomers among the screened reactions (eq 8). Again, (*aS,R*)-**L8-H** is better, albeit moderately, and an 84% unoptimized ee was achieved for cyclohexene product **15**. In these two cases, the product absolute configurations were also assigned upon comparison of their specific rotations to literature data.<sup>18</sup>

With acetal **16** as the substrate, the gold-catalyzed cycloisomerization led to indanone product **17** upon hydrolysis in good yields (Scheme 4).<sup>19</sup> Interestingly, in this case, (*aR,R*)-

#### Scheme 4. Gold(I)-Catalyzed Enantioselective Carboalkoxylation of Alkyne



**L8-H** induced much higher enantiomeric excesses than that of its (*aS,R*) counterpart, in contrast to the trend observed in Table 1, Scheme 3, and eqs 5, 7 and 8, where the latter ligand was more effective in asymmetric induction. The configuration of **18** was assigned on the basis of chiral HPLC behavior comparable to that of the literature.<sup>19</sup>

These results reveal that both the attractive interaction and the steric repulsion outlined in Figure 4 can indeed provide asymmetric induction. In most cases, the chiral steric environment posed by (*aS,R*)-**L8-H** is more effective in controlling the stereochemical outcomes. However, in the case of Scheme 4, the development of a discrete oxocarbenium intermediate prior to the enantiodetermining step apparently allows better stereocontrol by the electronic mode, therefore affording a much higher ee in the case of (*aR,R*)-**L8-H**.

#### CONCLUSIONS

We have synthesized and characterized four new chiral bifunctional NHC ligands based on the imidazo[1,5-*a*]pyridine (ImPy) scaffold. These ligands possess a fluxional biaryl axis, a chiral center, and a remote alkylamino group. Upon coordination to Au(I), the rotation around the biaryl axis is hindered, but the equilibria between the atropisomers can be established upon moderate heating. Despite the semistable axial chirality, these gold complexes are demonstrated to induce chirality with a range of gold-catalyzed transformations, and enantiomeric excesses can reach 84%. Two modes of imparting asymmetry by these ligands are chiral steric hindrance and asymmetric electrostatic attraction, the choice of which is dictated by the ligand axial chirality and often leads to opposite asymmetric induction. In most cases, ligand (*aS,R*)-**L8-H** with its cyclohexyl group pointing to the reaction

site and hence posing a chiral steric environment is more effective in inducing chirality than its atropisomer (*aR,R*)-**L8-H**, which relies on electrostatic attraction for enantioselectivity.

#### ASSOCIATED CONTENT

##### Supporting Information

The Supporting Information is available free of charge on the ACS Publications website at DOI: 10.1021/acs.organo-  
met.9b00400.

General procedures, procedure for the preparation of gold complexes, Au-catalyzed enantioselective transformations, X-ray structures of gold catalysts, <sup>1</sup>H and <sup>13</sup>C NMR spectra, HPLC chromatograms, and references (PDF)

#### Accession Codes

CCDC 1910598 and 1913712 contain the supplementary crystallographic data for this paper. These data can be obtained free of charge via [www.ccdc.cam.ac.uk/data\\_request/cif](http://www.ccdc.cam.ac.uk/data_request/cif), or by emailing [data\\_request@ccdc.cam.ac.uk](mailto:data_request@ccdc.cam.ac.uk), or by contacting The Cambridge Crystallographic Data Centre, 12 Union Road, Cambridge CB2 1EZ, UK; fax: +44 1223 336033.

#### AUTHOR INFORMATION

##### Corresponding Author

\*E-mail: [zhang@chem.ucsb.edu](mailto:zhang@chem.ucsb.edu).

##### ORCID

Yunkui Liu: 0000-0001-8614-458X

Xing-Wang Wang: 0000-0002-6004-8458

Liming Zhang: 0000-0002-5306-1515

##### Notes

The authors declare no competing financial interest.

#### ACKNOWLEDGMENTS

J.-Q.Z. and Y.L. thank the China Scholarship Council for a scholarship. The authors are thankful for National Institute of General Medical Sciences Grant R01GM123342 and National Science Foundation Grant CHE 1800525 for financial support and National Institutes of Health Shared Instrument Grant S10OD012077 for the purchase of a 400 MHz NMR spectrometer.

#### REFERENCES

- (1) (a) Cheng, X.; Wang, Z.; Quintanilla, C. D.; Zhang, L. Chiral Bifunctional Phosphine Ligand Enabling Gold-Catalyzed Asymmetric Isomerization of Alkyne to Allene and Asymmetric Synthesis of 2,5-Dihydrofuran. *J. Am. Chem. Soc.* **2019**, *141*, 3787–3791. (b) Liao, S.; Porta, A.; Cheng, X.; Ma, X.; Zanoni, G.; Zhang, L. Bifunctional Ligand Enables Efficient Gold-Catalyzed Hydroalkenylation of Propargylic Alcohol. *Angew. Chem., Int. Ed.* **2018**, *57*, 8250–8254. (c) Li, T.; Zhang, L. Bifunctional Biphenyl-2-Ylphosphine Ligand Enables Tandem Gold-Catalyzed Propargylation of Aldehyde and Unexpected Cycloisomerization. *J. Am. Chem. Soc.* **2018**, *140*, 17439–17443. (d) Wang, Z.; Ying, A.; Fan, Z.; Hervieu, C.; Zhang, L. Tertiary Amino Group in Cationic Gold Catalyst: Tethered Frustrated Lewis Pairs That Enable Ligand-Controlled Regiodivergent and Stereoselective Isomerizations of Propargylic Esters. *ACS Catal.* **2017**, *7*, 3676–3680. (e) Wang, Z.; Nicolini, C.; Hervieu, C.; Wong, Y.-F.; Zanoni, G.; Zhang, L. Remote Cooperative Group Strategy Enables Ligands for Accelerative Asymmetric Gold Catalysis. *J. Am. Chem. Soc.* **2017**, *139*, 16064–16067. (f) Li, X.; Wang, Z.; Ma, X.; Liu, P.-n.; Zhang, L. Designed Bifunctional Phosphine Ligand-Enabled Gold-Catalyzed Isomerizations of Ynamides and Allenamides: Stereoselective and Regioselective Formation of 1-Amido-1,3-

- Dienes. *Org. Lett.* **2017**, *19*, 5744–5747. (g) Li, X.; Liao, S.; Wang, Z.; Zhang, L. Ligand-Accelerated Gold-Catalyzed Addition of in Situ Generated Hydrazoic Acid to Alkynes under Neat Conditions. *Org. Lett.* **2017**, *19*, 3687–3690. (h) Wang, Z.; Wang, Y.; Zhang, L. Soft Propargylic Deprotonation: Designed Ligand Enables Au-Catalyzed Isomerization of Alkynes to 1,3-Dienes. *J. Am. Chem. Soc.* **2014**, *136*, 8887–8890. (i) Wang, Y.; Wang, Z.; Li, Y.; Wu, G.; Cao, Z.; Zhang, L. A General Ligand Design for Gold Catalysis Allowing Ligand-Directed Anti-Nucleophilic Attack of Alkynes. *Nat. Commun.* **2014**, *5*, 3470 DOI: 10.1038/ncomms4470.
- (2) (a) Hashmi, A. S. K. Sub-Nanosized Gold Catalysts. *Science* **2012**, *338*, 1434–1434. (b) Blanco Jaimes, M. C.; Rominger, F.; Pereira, M. M.; Carrilho, R. M. B.; Carabineiro, S. A. C.; Hashmi, A. S. K. Highly Active Phosphite Gold(I) Catalysts for Intramolecular Hydroalkoxylation, Enyne Cyclization and Furanyne Cyclization. *Chem. Commun.* **2014**, *50*, 4937–4940. (c) Blanco Jaimes, M. C.; Böhlring, C. R. N.; Serrano-Becerra, J. M.; Hashmi, A. S. K. Highly Active Mononuclear Nac–Gold(I) Catalysts. *Angew. Chem., Int. Ed.* **2013**, *52*, 7963–7966.
- (3) Alcarazo, M.; Roseblade, S. J.; Cowley, A. R.; Fernández, R.; Brown, J. M.; Lassaletta, J. M. Imidazo[1,5-a]Pyridine: A Versatile Architecture for Stable N-Heterocyclic Carbenes. *J. Am. Chem. Soc.* **2005**, *127*, 3290–3291.
- (4) Burstein, C.; Lehmann, C. W.; Glorius, F. Imidazo[1,5-a]Pyridine-3-Ylidenes—Pyridine Derived N-Heterocyclic Carbene Ligands. *Tetrahedron* **2005**, *61*, 6207–6217.
- (5) (a) Dinda, J.; Samanta, T.; Nandy, A.; Saha, K. D.; Seth, S. K.; Chattopadhyay, S. K.; Bielawski, C. W. N-Heterocyclic Carbene Supported Au(I) and Au(III) Complexes: A Comparison of Cytotoxicities. *New J. Chem.* **2014**, *38*, 1218–1224. (b) Rana, B. K.; Nandy, A.; Bertolasi, V.; Bielawski, C. W.; Das Saha, K.; Dinda, J. Novel Gold (I)–and Gold (III)–N-Heterocyclic Carbene Complexes: Synthesis and Evaluation of Their Anticancer Properties. *Organometallics* **2014**, *33*, 2544–2548.
- (6) (a) Kriechbaum, M.; List, M.; Berger, R. J. F.; Patzschke, M.; Monkowius, U. Silver and Gold Complexes with a New 1,10-Phenanthroline Analogue N-Heterocyclic Carbene: A Combined Structural, Theoretical, and Photophysical Study. *Chem. - Eur. J.* **2012**, *18*, 5506–5509. (b) Kriechbaum, M.; Winterleitner, G.; Gerisch, A.; List, M.; Monkowius, U. Synthesis, Characterization and Luminescence of Gold Complexes Bearing an Nhc Ligand Based on the Imidazo[1,5-a]Quinolinol Scaffold. *Eur. J. Inorg. Chem.* **2013**, *2013*, 5567–5575.
- (7) (a) Kim, Y.; Kim, Y.; Hur, M. Y.; Lee, E. Efficient Synthesis of Bulky N-Heterocyclic Carbene Ligands for Coinage Metal Complexes. *J. Organomet. Chem.* **2016**, *820*, 1–7. (b) Grande-Carmona, F.; Iglesias-Sigüenza, J.; Álvarez, E.; Díez, E.; Fernández, R.; Lassaletta, J. M. Synthesis and Characterization of Axially Chiral Imidazoisoquinolin-2-Ylidene Silver and Gold Complexes. *Organometallics* **2015**, *34*, 5073–5080. (c) Espina, M.; Rivilla, I.; Conde, A.; Díaz-Requejo, M. M.; Pérez, P. J.; Álvarez, E.; Fernández, R.; Lassaletta, J. M. Chiral, Sterically Demanding N-Heterocyclic Carbenes Fused into a Heterobiaryl Skeleton: Design, Synthesis, and Structural Analysis. *Organometallics* **2015**, *34*, 1328–1338.
- (8) (a) Alcarazo, M.; Stork, T.; Anoop, A.; Thiel, W.; Fürstner, A. Steering the Surprisingly Modular  $\pi$ -Acceptor Properties of N-Heterocyclic Carbenes: Implications for Gold Catalysis. *Angew. Chem., Int. Ed.* **2010**, *49*, 2542–2546. (b) Tang, Y.; Benaissa, I.; Huynh, M.; Vendier, L.; Lugan, N.; Bastin, S.; Belmont, P.; César, V.; Michelet, V. An Original L-Shape, Tunable N-Heterocyclic Carbene Platform for Efficient Gold(I) Catalysis. *Angew. Chem., Int. Ed.* **2019**, *58*, 7977–7981.
- (9) (a) Tao, W.; Wang, X.; Ito, S.; Nozaki, K. Palladium Complexes Bearing an N-Heterocyclic Carbene–Sulfonamide Ligand for Coo-igomerization of Ethylene and Polar Monomers. *J. Polym. Sci., Part A: Polym. Chem.* **2019**, *57*, 474–477. (b) Roseblade, S. J.; Ros, A.; Monge, D.; Alcarazo, M.; Alvarez, E.; Lassaletta, J. M.; Fernández, R. Imidazo[1,5-a]Pyridin-3-Ylidene/Thioether Mixed C/S Ligands and Complexes Thereof. *Organometallics* **2007**, *26*, 2570–2578. (c) Nakanano, R.; Nozaki, K. Copolymerization of Propylene and Polar Monomers Using Pd/Izqo Catalysts. *J. Am. Chem. Soc.* **2015**, *137*, 10934–10937.
- (10) Park, D.-A.; Ryu, J. Y.; Lee, J.; Hong, S. Bifunctional N-Heterocyclic Carbene Ligands for Cu-Catalyzed Direct C–H Carboxylation with Co<sub>2</sub>. *RSC Adv.* **2017**, *7*, 52496–52502.
- (11) Azouzi, K.; Duhayon, C.; Benaissa, I.; Lugan, N.; Canac, Y.; Bastin, S.; César, V. Bidentate Iminophosphorane-Nhc Ligand Derived from the Imidazo[1,5-a]Pyridin-3-Ylidene Scaffold. *Organometallics* **2018**, *37*, 4726–4735.
- (12) For selected reviews, see: (a) Zi, W.; Dean Toste, F. Recent Advances in Enantioselective Gold Catalysis. *Chem. Soc. Rev.* **2016**, *45*, 4567–4589. (b) Pradal, A.; Toullec, P. Y.; Michelet, V. Recent Developments in Asymmetric Catalysis in the Presence of Chiral Gold Complexes. *Synthesis* **2011**, *2011*, 1501–1514. (c) Sengupta, S.; Shi, X. Recent Advances in Asymmetric Gold Catalysis. *ChemCatChem* **2010**, *2*, 609–619. (d) Li, Y.; Li, W.; Zhang, J. Gold-Catalyzed Enantioselective Annulations. *Chem. - Eur. J.* **2017**, *23*, 467–512.
- (13) (a) Mendez, M.; Munoz, M. P.; Echavarren, A. M. Platinum-Catalyzed Alkoxy- and Hydroxycyclization of Enynes. *J. Am. Chem. Soc.* **2000**, *122*, 11549–11550. (b) Charruault, L.; Michelet, V.; Taras, R.; Gladiali, S.; Genet, J.-P. Functionalized Carbo- and Heterocycles Via Pt-Catalyzed Asymmetric Alkoxy cyclization of 1,6-Enynes. *Chem. Commun.* **2004**, 850–851. (c) Nieto-Oberhuber, C.; Munoz, M. P.; Bunuel, E.; Nevado, C.; Cardenas, D. J.; Echavarren, A. M. Cationic Gold(I) Complexes: Highly Alkynophilic Catalysts for the Exo- and Endo-Cyclization of Enynes. *Angew. Chem., Int. Ed.* **2004**, *43*, 2402–2406. (d) Pradal, A.; Chao, C.-M.; Vitale, M. R.; Toullec, P. Y.; Michelet, V. Asymmetric Au-Catalyzed Domino Cyclization/Nucleophile Addition Reactions of Enynes in the Presence of Water, Methanol and Electron-Rich Aromatic Derivatives. *Tetrahedron* **2011**, *67*, 4371–4377.
- (14) (a) Davies, H. M. L.; Antoulinakis, E. G. Intermolecular Metal-Catalyzed Carbenoid Cyclopropanations. *Org. React.* **2001**, *57*, 1–326. (b) Bertilsson, S. K.; Andersson, P. G. A Rigid Dirhodium(II) Carboxylate as an Efficient Catalyst for the Asymmetric Cyclopropanation of Olefins. *J. Organomet. Chem.* **2000**, *603*, 13–17. (c) Starmans, W. A. J.; Thijs, L.; Zwanenburg, B. Novel Chiral Dirhodium Catalysts Derived from Aziridine- and Azetidincarboxylic Acid for Intermolecular Cyclopropanation Reactions with Methyl Phenyl diazoacetate. *Tetrahedron* **1998**, *54*, 629–636. (d) Davies, H. M. L.; Rusiniak, L. Effect of Catalyst on the Diastereoselectivity of Methyl Phenyl diazoacetate Cyclopropanations. *Tetrahedron Lett.* **1998**, *39*, 8811–8812.
- (15) Prieto, A.; Fructos, M. R.; Mar Díaz-Requejo, M.; Pérez, P. J.; Pérez-Galán, P.; Delpont, N.; Echavarren, A. M. Gold-Catalyzed Olefin Cyclopropanation. *Tetrahedron* **2009**, *65*, 1790–1793.
- (16) (a) Cao, Z.-Y.; Wang, X.; Tan, C.; Zhao, X.-L.; Zhou, J.; Ding, K. Highly Stereoselective Olefin Cyclopropanation of Diazoindoles Catalyzed by a C<sub>2</sub>-Symmetric Spiroketal Bisphosphine/Au(I) Complex. *J. Am. Chem. Soc.* **2013**, *135*, 8197–8200. (b) Briones, J. F.; Davies, H. M. L. Gold(I)-Catalyzed Asymmetric Cyclopropanation of Internal Alkynes. *J. Am. Chem. Soc.* **2012**, *134*, 11916–11919. (c) Qian, D.; Hu, H.; Liu, F.; Tang, B.; Ye, W.; Wang, Y.; Zhang, J. Gold(I)-Catalyzed Highly Diastereo- and Enantioselective Alkyne Oxidation/Cyclopropanation of 1,6-Enynes. *Angew. Chem., Int. Ed.* **2014**, *53*, 13751–13755. (d) Ji, K.; Zheng, Z.; Wang, Z.; Zhang, L. Enantioselective Oxidative Gold Catalysis Enabled by a Designed Chiral P,N-Bidentate Ligand. *Angew. Chem., Int. Ed.* **2015**, *54*, 1245–1249. (e) Klimczyk, S.; Misale, A.; Huang, X.; Maulide, N. Dimeric Taddol Phosphoramidites in Asymmetric Catalysis: Domino Deracemization and Cyclopropanation of Sulfonium Ylides. *Angew. Chem., Int. Ed.* **2015**, *54*, 10365–10369.
- (17) García-Morales, C.; Ranieri, B.; Escofet, I.; López-Suarez, L.; Obradors, C.; Kononov, A. I.; Echavarren, A. M. Enantioselective Synthesis of Cyclobutenes by Intermolecular [2 + 2] Cycloaddition with Non-C<sub>2</sub> Symmetric Digold Catalysts. *J. Am. Chem. Soc.* **2017**, *139*, 13628–13631.

(18) (a) Hu, H.; Wang, Y.; Qian, D.; Zhang, Z.-M.; Liu, L.; Zhang, J. Enantioselective Gold-Catalyzed Intermolecular [2+ 2]-Cycloadditions of 3-Styrylindoles with N-Allenyl Oxazolidinone. *Org. Chem. Front.* **2016**, *3*, 759–763. (b) Huang, W.; Zhang, Y.-C.; Jin, R.; Chen, B.-L.; Chen, Z. Synthesis of Axially Chiral 1,2,3-Triazol-5-Ylidene–Au(I) Complex and Its Application in Enantioselective [2 + 2] Cycloaddition of Alleneamides with Alkenes. *Organometallics* **2018**, *37*, 3196–3209. (c) Jia, M.; Monari, M.; Yang, Q.-Q.; Bandini, M. Enantioselective Gold Catalyzed Dearomative [2 + 2]-Cycloaddition between Indoles and Allenamides. *Chem. Commun.* **2015**, *51*, 2320–2323. (d) Francos, J.; Grande-Carmona, F.; Faustino, H.; Iglesias-Sigüenza, J.; Díez, E.; Alonso, I.; Fernández, R.; Lassaletta, J. M.; López, F.; Mascareñas, J. L. Axially Chiral Triazoloisoquinolin-3-Ylidene Ligands in Gold(I)-Catalyzed Asymmetric Intermolecular (4 + 2) Cycloadditions of Allenamides and Dienes. *J. Am. Chem. Soc.* **2012**, *134*, 14322–14325.

(19) Zi, W.; Toste, F. D. Gold(I)-Catalyzed Enantioselective Carboalkoxylation of Alkynes. *J. Am. Chem. Soc.* **2013**, *135*, 12600–12603.